J. Fluid Mech. (1987), *vol.* 185, *pp.* 121–136
Printed in Great Britain

On the genesis of quasi-steady vortices in a rotating turbulent flow

By MATHIEU MORY AND PHILIPPE CAPERAN
Institut de Mécanique de Grenoble, Domaine Universitaire, BP 68,
38402 Saint Martin d'Hères Cédex, France

(Received 26 June 1986 and in revised form 12 May 1987)

Turbulent flows subjected to rotation display vortices parallel to the rotation axis and exhibiting a long timescale compared to the turbulent turnover time and the rotation period. A similar flow pattern is observed arising from the thermal instability in a rotating fluid. We demonstrate the analogy between turbulence and thermal convection in a rotating fluid. A basic quasi-geostrophic turbulent flow is considered which is forced at the bottom of the layer by a stochastic component of velocity parallel to the rotation axis. The turbulent basic state has no mean flow and the gradient along the rotation axis of the turbulent kinetic energy $-\partial_z\langle w^2\rangle$ is analogous to the mean temperature profile in thermal convection. The linear perturbation equations of this basic turbulent state are given, where the thermal diffusion equation is replaced by the turbulent kinetic energy equation. Using a simple closure of this equation the model demonstrates the occurrence of an instability when the Reynolds number exceeds a critical value. Marginal stability curves are deduced by numerical integration of the perturbation equations. The results show order-of-magnitude agreement with laboratory experiments.

1. Introduction

A number of experiments on turbulent flows subjected to rapid rotation have demonstrated the drastic effect of rotation on the structure of turbulence (Bretherton & Turner 1968; Colin de Verdière 1980; Hopfinger, Browand & Gagne 1982; Dickinson & Long 1982). When turbulence is continuously forced, as in the previously cited experiments, the flow tends to become two-dimensional in a plane perpendicular to the rotation axis. The flow pattern takes the form of an array of vortices that are roughly parallel to the rotation axis. These vortices possess a surprising degree of steadiness since their evolution timescale is large compared to the turbulence turnover time, and they have a well-defined lengthscale (no continuous growth in lengthscale according to the two-dimensional inverse cascade theory is observed).

The initiation of cyclones in a turbulent rotating fluid was interpreted by Scorer (1966) primarily as a process of angular-momentum mixing. This idea was further investigated by Bretherton & Turner (1968), McEwan (1976) and Thompson (1979), but it failed to predict the lengthscale of the vortices and to explain their long timescale. Another model of the initiation of cyclones was proposed by Maxworthy, Hopfinger & Redekopp (1985) using the analogy with stratified fluids. This mechanism does not lead to quantitative predictions either and its relevance needs to be confirmed by experiments. Lundgren (1985) has recently studied different

models of vortices in a rotating flow subjected to a slow withdrawal along the rotation axis and the results have been compared with observations by Hopfinger *et al.* (1982). Nevertheless, we believe that the continuous withdrawal assumption is a very restrictive one which itself implies that vortex genesis effect.

The present paper was motivated by a qualitative analogy between thermal convection and turbulence in a rotating fluid that appears when comparing the visualizations by Nakagawa & Frenzen (1955) and Hopfinger *et al.* (1982). The theoretical underpinnings of this analogy are examined. In §2 a quasi-geostrophic homogeneous turbulent flow is described which serves as the basic state of a flow whose linear stability is studied in §3. This turbulent flow is forced at the bottom of the layer by a stochastic component of velocity parallel to the rotation axis. The basic turbulent flow has no mean flow, and the averaged momentum equations show that the gradient along the axis of rotation of the turbulent kinetic energy $-\partial_z\langle w^2\rangle$ is equivalent to the mean temperature profile in thermal convection with rotation. The presentation of the stability analysis in §3 closely follows Chandrasekhar's (1961, §§24–29) presentation of thermal convection theory in order to highlight the similarities and place greater emphasis on the differences. Finally, §4 discusses the results of the theory in the context of the experiments of Colin de Verdière (1980) and Hopfinger *et al.* (1982, hereinafter referred to as HBG).

Our model of vortex genesis in a turbulent flow is complementary to the approach by Maxworthy *et al.* (1985) who considered the transient evolution once turbulence is suddenly produced in a rotating fluid. We do not examine the transient evolution but instead focus on the steady instability pattern of an established quasi-geostrophic turbulent flow having no mean flow component. We believe that this flow pattern is the one toward which the transient flow described by Maxworthy *et al.* will evolve. Since the basic turbulent flow is quasi-geostrophic, it is two-dimensional in a plane perpendicular to the rotation axis, implying an infinite speed of propagation of turbulent motions by inertial waves. This substantial simplification is presumably valid for averaged momentum equations. Nevertheless, the effect of inertial waves on the perturbation is taken into account in the perturbation equations derived in §3, although it vanishes when seeking steady solutions.

2. Basic state of boundary forced turbulence

Consider a geostrophic turbulent flow in a layer which is contained between the planes $z = -H$ and $z = 0$ (figure 1). The whole system is rotating around the z-axis with a Coriolis parameter $f = 2\Omega$. The dominant balance is between the Coriolis force and the pressure gradient,

$$\left.\begin{aligned} -f\rho v &\approx -\partial_x p, \\ f\rho u &\approx \partial_y p \end{aligned}\right\} \tag{2.1}$$

(see, for instance, the review by Rhines 1979 on geostrophic turbulence). This balance requires that the Rossby number ($Ro = \mathscr{U}/fL$) and the Ekman number ($E = \nu/fH^2$) are small. $\mathscr{U}$ is a representative velocity of motions in the plane (x, y), L is the horizontal lengthscale and H the vertical lengthscale (we assume the timescale to be $L/\mathscr{U}$). The continuity equation implies that the vertical component of velocity w scales with $Ro\,\mathscr{U}H/L$. Assuming $Ro^2H^2/L^2 \ll 1$ the pressure is nearly hydrostatic. From (2.1) the velocities u and v are independent of the z-coordinate and the

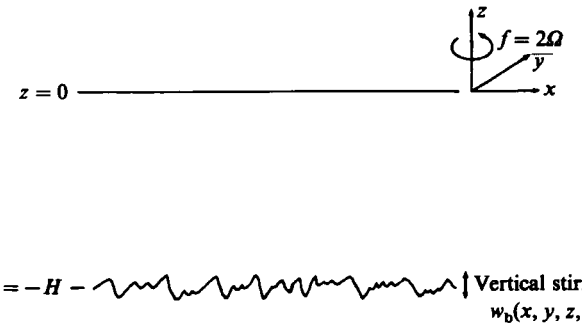

FIGURE 1. Schematic of the fluid layer in the coordinate system (O, x, y, z). The upper boundary $(z = 0)$ is rigid. The layer is stirred by a stochastically forced vertical component of velocity $w_b(x, y, t)$ at the lower boundary $(z = -H)$. The whole system is rotating and motions are quasi-geostrophic.

horizontal flow is two-dimensional. The time evolution of the geostrophic flow is given by the vorticity equation (Pedlosky 1979, p. 35)

$$(\partial_t + u\,\partial_x + v\,\partial_y)(\partial_x v - \partial_y u) = f\partial_z w + O\left(\frac{Ro\,\mathscr{U}^2}{L^2}, \frac{E\mathscr{U}^2}{L^2}\right). \tag{2.2}$$

The lowest-order term $O(\mathscr{U}^2/L^2)$ in the latter equation is independent of the z-coordinate. Hence, the rate of stretching $f\partial_z w$ is a function only of x, y and t. In our model the upper boundary is at rest ($w = 0$ for $z = 0$) but the lower boundary $(z = -H)$ experiences a vertical stirring with vertical velocity $w_b(x, y, t)$. Thus,

$$w(x, y, z, t) = -w_b(x, y, t)\frac{z}{H}. \tag{2.3}$$

In what follows, we shall only deal with Reynolds equations. If $\langle\ \rangle$ denotes the ensemble average, these equations are written in the rotating frame as

$$\partial_t\langle u\rangle + \partial_x\langle u^2\rangle + \partial_y\langle uv\rangle + \partial_z\langle uw\rangle - f\langle v\rangle = \frac{1}{\rho}\partial_x\langle p\rangle + \nu\Delta\langle u\rangle, \tag{2.4a}$$

$$\partial_t\langle v\rangle + \partial_x\langle uv\rangle + \partial_y\langle v^2\rangle + \partial_z\langle vw\rangle + f\langle u\rangle = -\frac{1}{\rho}\partial_y\langle p\rangle + \nu\Delta\langle v\rangle, \tag{2.4b}$$

$$\partial_t\langle w\rangle + \partial_x\langle uw\rangle + \partial_y\langle vw\rangle + \partial_z\langle w^2\rangle = -\frac{1}{\rho}\partial_z\langle p\rangle + \nu\Delta\langle w\rangle. \tag{2.4c}$$

The flow is assumed to be fully turbulent and it has no mean component, implying

$$\langle u\rangle = \langle v\rangle = \langle w\rangle = 0. \tag{2.5}$$

The forcing by the vertical component of velocity $w_b(x, y, t)$ at the bottom boundary is stochastic both in time and space and we assume that it is stationary and homogeneous,

$$\partial_t\langle w_b^2\rangle = \partial_x\langle w_b^2\rangle = \partial_y\langle w_b^2\rangle = 0. \tag{2.6}$$

As a consequence, turbulence is supposed to be statistically stationary and we assume that the geostrophic flow is homogeneous,

$$\partial_t\langle u^2\rangle = \partial_t\langle v^2\rangle = \partial_x\langle u^2\rangle = \partial_x\langle v^2\rangle = \partial_y\langle u^2\rangle = \partial_y\langle v^2\rangle = 0. \tag{2.7}$$

When turbulence has been established the vertical motions are no longer statistically correlated with the horizontal motions, and any turbulent vortex can be either stretched or compressed. We obtain

$$\langle uv \rangle = \langle uw \rangle = \langle vw \rangle = 0. \tag{2.8}$$

All terms in the momentum equations (2.4) vanish except for the momentum on the z-axis which reduces to

$$\partial_z \langle w^2 \rangle = -\frac{1}{\rho} \partial_z \langle p \rangle. \tag{2.9}$$

The vertical gradient of the turbulent kinetic energy is

$$\partial_z \langle w^2 \rangle = 2 \frac{\langle w_b^2(x, y, t) \rangle}{H^2} z = 2\beta z \tag{2.10}$$

as deduced from (2.3). This quantity is not zero and it has to be balanced by a vertical mean pressure gradient†. The particular form of the quantity $-\partial_z \langle w^2 \rangle$ has to be emphasized. Its behaviour is similar to the basic temperature profile in Rayleigh–Bénard convection ($\bar{T} = -\beta z$). The vertical gradient ($-\partial_{zz} \langle w^2 \rangle = -2\beta$) is constant and negative like the mean temperature gradient in a thermal convection system. The linear stability of the turbulent flow described above is investigated in the following section.

The framework of quasi-geostrophic turbulence is chosen for its physical significance as a classical kind of flow occurring in rotating fluids. A consequence of the quasi-geostrophic approximation is that $\partial_{zz} \langle w^2 \rangle$ is uniform through the fluid. Quasi-geostrophy has no further implication in the stability analysis presented below, which is valid for any turbulent flow, which verifies the statistical relationships (2.5)–(2.10). However, quasi-geostrophy implies that vertical velocities are smaller than horizontal velocities by a factor $Ro\,H/L$. We show in the next section that the convection pattern has to verify a similar constraint and we specify the conditions under which it holds.

3. The perturbation analysis

3.1. *The perturbation equations*

We denote by (U, V, W, P) a perturbation of the flow field which is superimposed on the turbulent field (u, v, w, p). We seek unstable perturbations, i.e. perturbations that will grow in time. The timescale of these perturbations is assumed to be large compared to the turbulent turnover time. This assumption is necessary in order to distinguish the perturbation (U, V, W, P) from the turbulent motions. Writing the turbulent flow field, as perturbed by (U, V, W, P), as (u', v', w', p'), the instantaneous components of velocity are then $U+u'$, $V+v'$, $W+w'$, and the pressure is $P+p'$. However, we need only consider the statistically averaged quantities appearing in the Reynolds equations. (U, V, W) being the mean component of the flow field, we obtain

$$\langle u' \rangle = \langle v' \rangle = \langle w' \rangle = 0. \tag{3.1}$$

† In the framework of geostrophic flows (see Pedlosky 1979 for instance) the momentum equations are expanded to the different orders of the Rossby number. Geostrophy, (2.1), is the zeroth order, (2.2) corresponds to the first order, whereas (2.9) is the second order. In principle the correlations $\langle uw \rangle$ and $\langle vw \rangle$ include higher orders of perturbations of the geostrophic flow which are assumed to be zero from (2.8).

Furthermore, we assume that all statistical quantities that were spatially homogeneous without the perturbation will remain homogeneous in the presence of the perturbation. Reasons for this considerable simplification are discussed below. Equations (2.7) and (2.8) then imply

$$\partial_x\langle u'^2\rangle = \partial_y\langle u'^2\rangle = \partial_x\langle v'^2\rangle = \partial_y\langle v'^2\rangle = \langle u'v'\rangle = \langle u'w'\rangle = \langle v'w'\rangle = 0. \quad (3.2)$$

On the other hand $\langle w^2\rangle$ is not homogeneous (see (2.10)), and we should expect the quantity $\langle w'^2\rangle$ to diverge from $\langle w^2\rangle$ because fluid particles are convected within the layer. Denoting this departure as

$$\phi = \langle w'^2\rangle - \langle w^2\rangle = \langle w'^2\rangle - \beta z^2, \quad (3.3)$$

this quantity is not spatially homogeneous in general, i.e.

$$\partial_x\phi \not\equiv 0, \quad \partial_y\phi \not\equiv 0, \quad \partial_z\phi \not\equiv 0. \quad (3.4)$$

The modification of the turbulent averaged quantities by the perturbation appears in the Reynolds equations only through ϕ as a result of (3.2) and (3.4). ϕ is assumed to be of the order of magnitude of the linear part of the momentum of the perturbation (U, V, W, P). The momentum equations are simplified by statistical averaging of all turbulent quantities. We obtain

$$\partial_t U + U\partial_x U + V\partial_y U + W\partial_z U - fV = -\frac{1}{\rho}\partial_x P + \nu\Delta U, \quad (3.5)$$

$$\partial_t V + U\partial_x V + V\partial_y V + W\partial_z V + fU = -\frac{1}{\rho}\partial_y P + \nu\Delta V, \quad (3.6)$$

$$\partial_t W + U\partial_x W + V\partial_y W + W\partial_z W + \partial_z\langle w'^2\rangle = -\frac{1}{\rho}\partial_z P + \nu\Delta W, \quad (3.7)$$

where (3.1) and (3.2) have been applied. Subtracting (2.9) from (3.7) and using (3.3), ϕ appears in (3.7):

$$\partial_t W + U\partial_x W + V\partial_y W + W\partial_z W + \partial_z\phi = -\frac{1}{\rho}\partial_z(P - \langle p\rangle) + \nu\Delta W. \quad (3.8)$$

$P - \langle p\rangle$ is the mean pressure. Without restricting the generality of the problem $\langle p\rangle$ is incorporated in P in what follows. The linearized forms of (3.5), (3.6) and (3.8) with respect to U, V, W and P give the small-amplitude equations, namely

$$\partial_t U - fV = -\frac{1}{\rho}\partial_x P + \nu\Delta U, \quad (3.9)$$

$$\partial_t V + fU = -\frac{1}{\rho}\partial_y P + \nu\Delta V, \quad (3.10)$$

$$\partial_t W + \partial_z\phi = -\frac{1}{\rho}\partial_z P + \nu\Delta W. \quad (3.11)$$

Now with ζ the z-component of vorticity,

$$\zeta = \partial_x V - \partial_y U, \quad (3.12)$$

the time evolution of ζ is deduced from (3.9) and (3.10) as

$$\partial_t \zeta = f \partial_z W + \nu \Delta \zeta, \tag{3.13}$$

where the continuity equation

$$\partial_x U + \partial_y V + \partial_z W = 0 \tag{3.14}$$

has been used. On the other hand the pressure is expressed by applying the divergence operator to (3.9)–(3.11)

$$-\frac{1}{\rho}\Delta P = \partial_{zz}\phi - f\zeta, \tag{3.15}$$

and using the latter relation in (3.11) after the Laplacian operator has been applied to it leads to

$$\partial_t \Delta W = -f \partial_z \zeta + \nu \Delta\Delta W + (\partial_{xx} + \partial_{yy})\theta. \tag{3.16}$$

For convenience, the quantity

$$\theta = -\partial_z \phi(x, y, z, t) \tag{3.17}$$

has been introduced in (3.16), because (3.13) and (3.16) show a remarkable analogy with the Rayleigh–Bénard convection problem with rotation (see Chandrasekhar (1961), chap. III). The latter equations are the basic equations governing the time evolution of the vorticity and the velocity component along the rotation axis in thermal convection, θ denoting in this case the departure of temperature from the mean temperature profile. The time evolution of the temperature perturbation θ is given by the thermal diffusion equation,

$$\partial_t \theta - \beta w = \kappa \Delta \theta, \tag{3.18}$$

where β and κ are the mean temperature gradient and the thermal diffusivity, respectively. In the current turbulence problem we replace (3.18) by an equation which is deduced from the time-evolution equation of the turbulent kinetic energy of the z-component of velocity. This equation is written (see Monin & Yaglom 1965, p. 383)

$$\begin{aligned}(\partial_t + U\partial_x + V\partial_y + W\partial_z - \nu\Delta)\langle w'^2\rangle + 2\langle w'^2\rangle \partial_z W \\ = -\partial_x\langle u'w'^2\rangle - \partial_y\langle v'w'^2\rangle - \partial_z\langle w'^3\rangle - 2\langle (w'/\rho)\partial_z p'\rangle - 2\nu\langle \nabla w' \cdot \nabla w'\rangle.\end{aligned} \tag{3.19}$$

Terms on the right-hand side make the latter equation much more complex than the thermal diffusion equation and a closure theory is required. First notice that third-order correlations $\langle u'w'^2\rangle$, $\langle v'w'^2\rangle$ and $\langle w'^3\rangle$ vanish because probabilities for the sign of each velocity component being positive or negative are equal. When there is no mean flow (3.19) reduces to

$$-\nu\Delta\langle w^2\rangle = -2\langle (w/\rho)\partial_z p\rangle - 2\nu\langle \nabla w \cdot \nabla w\rangle. \tag{3.20}$$

Introducing $\phi = \langle w'^2\rangle - \langle w^2\rangle$ in (3.19) and linearizing with respect to U, V, W and ϕ, we obtain

$$\begin{aligned}(\partial_t - \nu\Delta)\phi + 2\langle w^2\rangle \partial_z W + \partial_z\langle w^2\rangle W \\ = -2(\langle (w'/\rho)\partial_z p'\rangle - \langle (w/\rho)\partial_z p\rangle) - 2\nu(\langle \nabla w' \cdot \nabla w'\rangle - \langle \nabla w \cdot \nabla w\rangle),\end{aligned} \tag{3.21}$$

where (3.20) has been used. The closure of the right-hand side of (3.21) should retain the turbulent diffusion of ϕ and some interaction between the turbulence and the mean flow through velocity–pressure correlations. The consistency of our linear model requires the closure of (3.21) to be a linear function of ϕ and W. We set

$$\begin{aligned}-2(\langle (w'/\rho)\partial_z p'\rangle - \langle (w/\rho)\partial_z p\rangle) - 2\nu(\langle \nabla w' \cdot \nabla w'\rangle - \langle \nabla w \cdot \nabla w\rangle) \\ = 2A\langle w^2\rangle \partial_z W + \nu_t \Delta\phi.\end{aligned} \tag{3.22}$$

A is a constant of order unity and ν_t denotes the turbulent diffusivity. Using (2.10) and (3.22), (3.21) leads to

$$(\partial_t - \kappa\Delta)\phi + 2\beta z W + 2\beta(1-A) z^2 \partial_z W = 0, \tag{3.23}$$

with $\kappa = \nu + \nu_t$. Applying the z-derivative to (3.23) gives the time evolution of θ. We get

$$(\partial_t - \kappa\Delta)\theta - 2\beta w - 2\beta(3-2A) z \partial_z W - 2(1-A)\beta z^2 \partial_{zz} W = 0. \tag{3.24}$$

This equation replaces the thermal diffusion equation (3.18). The linear system to be solved consists of (3.13), (3.16) and (3.24).

Returning to the assumption of no variation of the quantities $\langle u'^2\rangle$, $\langle v'^2\rangle$, $\langle u'v'\rangle$, $\langle u'w'\rangle$ and $\langle v'w'\rangle$ (see (3.2)), one notes that a complete solution of the problem involves the solution of the evolution equations for all components of the Reynolds stress tensor. This requires five additional closures for these equations. Since $\langle uv\rangle = \langle uw\rangle = \langle vw\rangle = 0$ in the basic state there should be no interaction between the mean flow and the Reynolds stresses, so that the equations (similar to (3.21)) reduce to simple diffusion equations for the quantities $\langle u'v'\rangle$, $\langle v'w'\rangle$ and $\langle u'w'\rangle$. It is therefore valid to neglect these terms. The same considerations cannot apply to $\langle u'^2\rangle$ and $\langle v'^2\rangle$. Since $\langle u^2\rangle \neq 0$ and $\langle v^2\rangle \neq 0$, interactions of turbulence with the mean flow can produce an accumulation of turbulent energy at some places. We omit this effect for simplicity, and conjecture that it has no crucial implication. Similarly, in §3.3 an output of the model will indicate that energy exchanges between $\langle w'^2\rangle$ and the mean flow is not a leading effect in the instability process.

3.2. *Normal mode analysis*

We seek solutions having the form

$$\left.\begin{aligned} W(x,y,z,t) &= W_1(z)\, \mathrm{e}^{\mathrm{i}(k_x x + k_y y) + pt}, \\ \theta(x,y,z,t) &= \Theta(z)\, \mathrm{e}^{\mathrm{i}(k_x x + k_y y) + pt}, \\ \zeta(x,y,z,t) &= Z(z)\, \mathrm{e}^{\mathrm{i}(k_x x + k_y y) + pt}. \end{aligned}\right\} \tag{3.25}$$

Equations (3.13), (3.16) and (3.24) become, respectively,

$$\{p - \nu(\mathrm{D}^2 - k^2)\} Z = f \mathrm{D} W_1, \tag{3.26}$$

$$\{p - \nu(\mathrm{D}^2 - k^2)\}(\mathrm{D}^2 - k^2) W_1 = -f \mathrm{D} Z - k^2 \Theta, \tag{3.27}$$

$$\{p - \kappa(\mathrm{D}^2 - k^2)\}\Theta = 2\beta W_1 + 2\beta(3-2A) z \mathrm{D} W_1 + 2\beta(1-A) z^2 \mathrm{D}^2 W_1, \tag{3.28}$$

with $k^2 = k_x^2 + k_y^2$ and $\mathrm{D} = \partial_z$. By applying the operator $(p - \kappa(\mathrm{D}^2 - k^2))(p - \nu(\mathrm{D}^2 - k^2))$ to (3.27) we obtain

$$\begin{aligned} \{p - \nu(\mathrm{D}^2 - k^2)\}^2 \{p - \kappa(\mathrm{D}^2 - k^2)\}(\mathrm{D}^2 - k^2) W_1 &= -f^2 \{p - \kappa(\mathrm{D}^2 - k^2)\} \mathrm{D}^2 W_1 \\ &\quad - 2\beta k^2 \{p - \nu(\mathrm{D}^2 - k^2)\}\{1 + (3-2A) z \mathrm{D} + (1-A) z^2 \mathrm{D}^2\} W_1, \end{aligned} \tag{3.29}$$

after (3.26) and (3.28) have been used. The system is unstable when one can find a value of p with $\mathrm{Re}\,(p) > 0$ such that (3.29) is satisfied together with associated boundary conditions. The system is of order eight. The order is reduced to six when instability sets in as stationary convection ($p = 0$). Equation (3.29) can then be written

$$-\nu^2 \kappa (\mathrm{D}^2 - k^2)^3 W_1 = f^2 \kappa \mathrm{D}^2 W_1 + 2\beta\nu k^2 \{1 + (3-2A) z \mathrm{D} + (1-A) z^2 \mathrm{D}^2\} W_1. \tag{3.30}$$

When the depth of the layer is chosen for the lengthscale the dimensionless wavenumber is defined as

$$a = kH, \tag{3.31}$$

and (3.30) can be rewritten in dimensionless form

$$(\mathrm{D}^2-a^2)^3 W_1 = -Ta\,\mathrm{D}^2 W_1 - Re\,a^2\{1+(3-2A)\,z\,\mathrm{D}+(1-A)\,z^2\,\mathrm{D}^2\}\,W_1. \quad (3.32)$$

There are two non-dimensional numbers in (3.32), namely the Taylor number as usually defined,

$$Ta = \frac{f^2 H^4}{\nu^2} = \frac{1}{E^2} \quad (3.33)$$

(E being the Ekman number defined in §2), and the Reynolds number

$$Re = \frac{2\beta H^4}{\nu\kappa}, \quad (3.34)$$

which is equivalent to the Rayleigh number in thermal convection. Incidentally an equivalent Prandtl number is $Pr = \nu/\kappa$. If the turbulent diffusivity of the turbulent kinetic energy is neglected ($\nu_t = 0$ in (3.22)) the Prandtl number is $Pr = 1$ as deduced from (3.24), and his number decreases for increasing eddy diffusivity.

Six boundary conditions are required to solve (3.32). Since the upper boundary ($z = 0$) is a solid wall the associated boundary conditions are

$$W_1 = \mathrm{D}W_1 = \phi = 0 \quad (3.35)$$

or

$$W_1 = \mathrm{D}^2 W_1 = \phi = 0, \quad (3.36)$$

depending on whether the upper boundary is rigid or free. The boundary condition on ϕ expresses the requirement of zero velocity component normal to the wall. The lower boundary ($z = -H$) is an open boundary where the turbulent velocity w is of maximum strength. Imposing the condition $W_1 = 0$ at $z = -H$ would imply that the rate of stretching, $\mathrm{D}W_1$, changes its sign between $z = 0$ and $z = -H$. At any point (x, y) the integrated vorticity ζ along the z-axis from $z = -H$ to $z = 0$ would then equal zero, suggesting a flow that consists of vortices with opposite moment on top of one other. This is seen, for instance, in the cell pattern of thermal convection as it is illustrated by Veronis (1959) and Chandrasekhar (1961, p. 113). In turbulent rotating flows, though, such vortex structures, imposed by the boundary condition $W_1 = 0$ at $z = -H$, are not observed. Since the lower boundary is not a wall, this condition can be relaxed. We instead pose

$$\mathrm{D}W_1 = 0, \quad (3.37a)$$

$$(\mathrm{D}^2+a^2)\,W_1 = 0, \quad (3.37b)$$

and

$$\phi = 0 \quad \text{at } z = -1 \quad (3.37c)$$

(z being dimensionless). The boundary conditions (3.37*a–c*) allow a mass exchange between the layer and the outside ($W_1 \neq 0$ at $z = -1$). However, there is no dynamical coupling between the two. Equation (3.37*c*) imposes the condition that the turbulent kinetic energy at the lower boundary remain unchanged when convection sets is. As a result of (3.37*a*) there is no energy exchange between the mean flow and the turbulence at this position, and (3.23) reduces to a balance of the turbulent kinetic energy flux with diffusion driven by the interior mean flow. Finally, (3.37*b*) expresses that the exterior flow applies no torque at the boundary. Indeed, Reynolds stresses apply no torque as a result of (3.2), and the transverse components of the viscous stress tensor vanish if

$$\mu(\partial_z U + \partial_x W) = 0, \quad (3.38a)$$

$$\mu(\partial_z V + \partial_y W) = 0. \quad (3.38b)$$

Using (3.38), the application of the z-derivative to (3.14) immediately leads to (3.37*b*). Succinctly, the flow between the layer and the exterior is driven by the internal dynamics of the layer. The exterior region only serves as an energy source. This is a major difference between our model and previous ones (Lundgren 1985; Maxworthy *et al.* 1985), which assumed that the generation of vortices was governed by motions parallel to the rotation axis. These vertical motions are an input in the latter models, whereas in our model they are a consequence of the dynamics of the layer.

The present theory was formulated in the context of laboratory experiments with large Taylor numbers (i.e. small Ekman numbers). We restrict ourselves to this case in what follows. We shall see that (3.32) reduces to an equation of order two, for which we shall retain only the two lowest-order boundary conditions,

$$W_1 = 0 \quad \text{at } z = 0, \qquad \mathrm{D}W_1 = 0 \quad \text{at } z = -1. \tag{3.39}$$

3.3. *Critical conditions at large Taylor numbers*

Provided a solution of (3.32) exists for asymptotically large Taylor numbers (i.e. $Ta \to \infty$), we expect that W_1 and its derivatives will not become disproportionately large. Equation (3.32) therefore reduces to a second-order differential equation with associated boundary conditions given by (3.39). The results on the existence of a solution for a Sturm–Liouville system (see Morse & Feshbach 1953, for instance) imply that a^6 and $Re\, a^2$ must be of the order of magnitude of Ta. We set

$$Re = rTa^{\frac{2}{3}}, \quad a = \alpha Ta^{\frac{1}{6}}. \tag{3.40}$$

Using this scaling, (3.32) reduces to

$$\{1 + r\alpha^2(1-A)z^2\}\,\mathrm{D}^2W_1 + r\alpha^2(3-2A)z\,\mathrm{D}W_1 + (r\alpha^2 - \alpha^6)W_1 = 0, \tag{3.41}$$

an equation that does not depend on the Taylor number. If r_m denotes the lowest value for which (3.41) admits a solution with a given value α_m, the critical Reynolds number Re_m and the corresponding wavenumber a_m are then $Re_\mathrm{m} = r_\mathrm{m}Ta^{\frac{2}{3}}$ and $a_\mathrm{m} = \alpha_\mathrm{m}Ta^{\frac{1}{6}}$, respectively. This number may not be the critical Reynolds number because the marginally unstable state is not necessarily stationary convection (i.e. $\mathrm{Im}(p) = 0$). However, there are reasons to believe that instability occurs via an exchange of stability. This happens in thermal convection when the Prandtl number is greater than or equal to 1 (Chandrasekhar 1961, §29). It was mentioned in §3.2 that the equivalent Prandtl number is $Pr = 1$ in our problem when turbulent diffusion is neglected. The similarity of (3.13), (3.16) and (3.24) with the equations of thermal convection may imply in certain cases a similar transition to instability. The possible existence of overstable oscillations for a Reynolds number below the critical value for stationary convection is not investigated in the present paper. However, future research should consider this more complicated case, especially as turbulent diffusion decreases the equivalent Prandtl number below $Pr = 1$.

The marginal curve of stability (i.e. $Re_\mathrm{m}/Ta^{\frac{2}{3}}$ as a function of $a_\mathrm{m}/Ta^{\frac{1}{6}}$) has been obtained by numerical integration of (3.41) for different values of A. A shooting technique was used. Eigenvalues $\lambda = \alpha^6 - r\alpha^2$ were computed for given values of $r\alpha^2$ and there is a non-zero physically meaningful solution to (3.41) when at least one eigenvalue corresponds to a positive value of α^6. The marginal curve of stability $r_\mathrm{m} = r_\mathrm{m}(\alpha_\mathrm{m})$ was determined as the lower curve bounding the domain containing the unstable points (there is no solution for $r < r_\mathrm{m}(\alpha_\mathrm{m})$). The existence of this curve is established when $A \leqslant 1$ because $(1 + r\alpha^2(1-A)z^2)$ is always positive and (3.41) is a

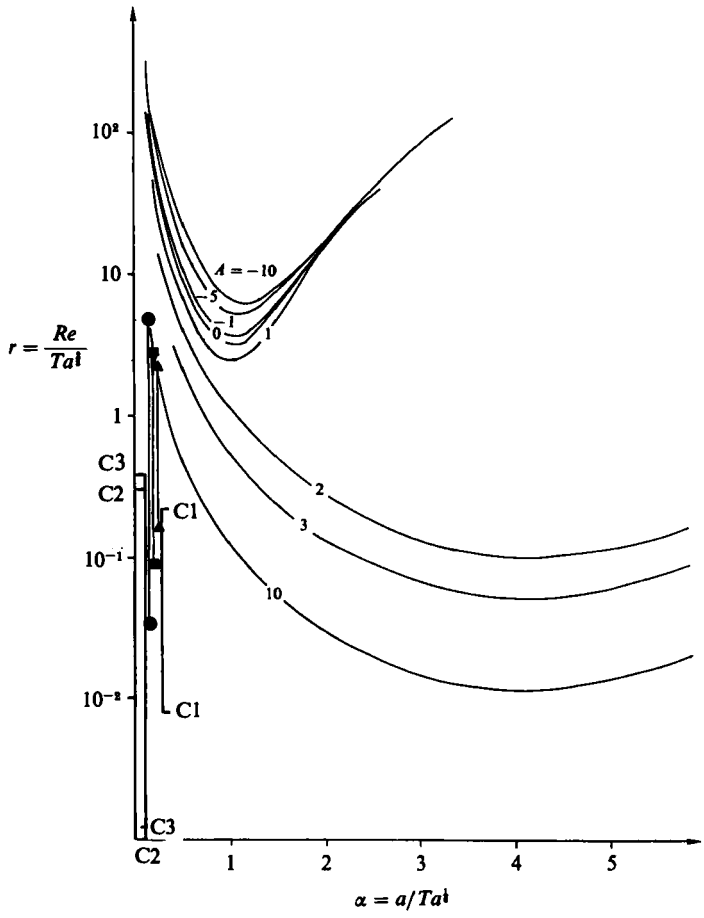

FIGURE 2. Marginal stability curves $r_m(\alpha_m)$ for various values of the parameter A. A logarithmic scale is used for the Reynolds number $Re/Ta^{\frac{1}{2}}$. For each curve the region below the curve corresponds to stable conditions. Error bars indicate the range of values accounting for three HBG experiments. For all experiments the grid oscillation frequency is $n = 13.3\,\pi$ rad s^{-1}. The Coriolis frequencies ($f = 2\Omega$) are 4π rad s^{-1} (▲), 2π rad s^{-1} (■) and $0.4\,\pi$ rad s^{-1} (●), respectively. The depth of the layer is $H = 50$ cm. The mesh and the stroke of the grid are $M = 5$ cm and $S = 4$ cm, respectively. Also plotted are the error bars (respectively C1, C2 and C3) which correspond to the three experiments reported in table 2 of Colin de Verdière's (1980) paper.

Sturm–Liouville eigenvalue problem of the form $\mathrm{D}(q_1(z)\,\mathrm{D}W_1) = \lambda q_2(z)\,W_1$, q_1 and q_2 being two positive and continuous functions in the range $-1 \leqslant z \leqslant 0$. The eigenvalues λ_i form an infinite set of negative numbers having an upper bound. When $A > 1$ the quantity $(1 + r\alpha^2(1-A)\,z^2)$ changes its sign between $z = -1$ and $z = 0$ unless $r\alpha^2$ is sufficiently small. Hence there also exists a marginal curve of stability when $A > 1$ though we may expect that this curve will be shifted towards smaller values of r for increasing values of A. This is most clearly seen in figure 2 where the marginal curves of stability are plotted for various values of A (recall that A parametrizes in the present model the energy transfers between the mean flow and turbulence). The plots are restricted to values of A ranging from -10 to 10, these being the most reasonable numbers for the purpose of discussing the experiments of HBG (see §4). When $A < -10$ or $A > 10$ the closure of the turbulent kinetic energy is presumably no longer satisfactory since this implies a high rate of energy exchange

between the mean flow and turbulence. A special case is $A = 1$. In this case (3.23) indicates the absence of interaction between the mean flow and turbulence. Perturbations of the turbulent kinetic energy are carried with the mean flow while diffusing. When A is not equal to 1 interactions between the mean flow and turbulence take place. The effect is weak for A decreasing from the value $A = 1$. The marginal curve of stability shifts slightly towards larger values of r without variation of the wavenumber band. On the contrary we verify that instability occurs for much lower values of r when A is increased above $A = 1$. In this case the wavenumber of the most unstable mode increases with increasing A.

The critical Reynolds number Re_c for a given value of A is determined in figure 2 from the lowest value r_c of the marginal curve of stability. Then

$$Re_c = r_c Ta^{\frac{1}{3}}, \tag{3.42}$$

and the corresponding wavenumber is

$$a_c = \alpha_c Ta^{\frac{1}{6}}. \tag{3.43}$$

α_c is the value of α_m corresponding to r_c on the marginal curve of stability. An interesting result of figure 2 is that α_c is ~ 1 for all values of A below $A = 1$ and therefore the scale of the most unstable mode only weakly depends on A.

It is worth noting that the mean flow is in geostrophic equilibrium at large Taylor numbers. The ratio of the viscous force to the Coriolis force is of order $Ta^{-\frac{1}{6}} a^2$, and it therefore decreases like $Ta^{-\frac{1}{6}}$ since $a^2 \sim Ta^{\frac{1}{3}}$, (3.40). The continuity equation then implies that the vertical velocities W have to be small compared with horizontal velocities (U, V). We verify this condition with (3.14) when $(\alpha/2\pi)^3 \ll 1$, this inequality holding at least for $\alpha \lesssim \alpha_c$.

4. The application to laboratory experiments

Turbulence in HBG experiments is generated by an oscillating grid in the lower part of the rotating tank. (The HBG experimental set-up is described summarily here. The reader may refer to their paper for further details.) Far from the grid midplane the flow consists of an array of vortices roughly parallel to the rotation axis. The flow is quasi two-dimensional in a plane perpendicular to this axis, and geostrophic except within the vortex cores. On the other hand, turbulence is only weakly modified by the rotational constraints in the region close to the grid where it is mainly three-dimensional. The transition between the regions with three-dimensional and two-dimensional turbulence is shown to be sharp (HBG). Hence straightforward choices for the positions $z = 0$ and $z = -H$ (see figure 1) are the upper boundary of the tank (a rigid lid in the experiment) and the position of the latter transition (referred to as Z_T in the HBG paper), respectively, so that H is approximately 50 cm. Streakline photographs of the flow in a sheet of light parallel to the rotation axis (Mory & Hopfinger 1985) confirm the quasi two-dimensionality of the flow, but they do not give quantitative estimates of the vertical component of velocity at the position $z = -H$ as defined by (2.3), not do they bear out the choice of H as vertical lengthscale. Two reasons for this may be mentioned. First, steady vortices were observed in all experiments that have been carried out. Velocity measurements could not be performed independently of the steady flow pattern. Secondly, streakline photographs give a correct measurement of the velocity only for particles remaining in the sheet of light during the whole exposure time. Owing to the horizontal motions, most particles cross the sheet of light during this time except in

the central part of the vortices where a strong component of velocity parallel to the rotation axis is measured. Therefore we only estimate an upper and a lower bound for the velocity $\langle w_b^2\rangle^{\frac{1}{2}}$ at the lower boundary ($z = -H$). The upper bound is given by taking $\langle w_b^2\rangle^{\frac{1}{2}} = u$, where u is the representative velocity of motions in a plane perpendicular to the rotation axis (see §2). This is a correct scaling in the domain where motions are three-dimensional and this scaling is an upper bound of the velocity scale in the transition region between three-dimensional and two-dimensional turbulence. Parameters that can be varied in HBG experiments are the rotation period of the tank $\Omega(f = 2\Omega)$, the frequency of grid oscillation n and the depth of the fluid. The results of HBG (§2 in their paper) lead to

$$\langle w_b^2\rangle^{\frac{1}{2}}_{\max} \sim u = 4.8\times 10^{-2}\,[S(SM)^{\frac{1}{2}}]^{\frac{1}{2}}(nf)^{\frac{1}{2}} \tag{4.1}$$

for the upper bound of $\langle w_b^2\rangle^{\frac{1}{2}}$, where M and S denote the mesh and the amplitude of oscillation of the grid, respectively. On the other hand the lower bound is determined from the geostrophic scaling of the vertical velocity (§2) based on the eddy spacing l_s,

$$\langle w_b^2\rangle^{\frac{1}{2}}_{\min} \sim fH\left(u/f\,l_s\right)^2 \sim 1.9\times 10^{-3}\,fH, \tag{4.2}$$

recalling that the Rossby number $(u/f\,l_s)$ is about 0.044 (HBG).

Figure 2 enables the present model of instability to be compared with the HBG experiments. The definitions of the Reynolds and Taylor numbers (3.33) and (3.34) and the asymptotic relationships between the Reynolds number, the wavenumber and the Taylor number lead to

$$r = 2\frac{\langle w_b^2\rangle H^2}{\nu^2}\left(\frac{\nu}{fH^2}\right)^{\frac{4}{3}} \tag{4.3}$$

and

$$\alpha = \frac{2\pi H}{l_s}\left(\frac{\nu}{fH^2}\right)^{\frac{1}{3}}, \tag{4.4}$$

where the wavenumber $k = 2\pi/l_s$ is related by (3.31) to the dimensionless wavenumber a. In (4.3) the eddy diffusivity ν_t has been neglected, and the diffusivity κ is then equal to the molecular diffusivity ν. The implications of this assumption are discussed later on. Replacing $\langle w_b^2\rangle$ by its maximum (4.1) and minimum (4.2) values, the upper and lower bounds of the value of r achieved in an experiment are

$$r_{\max} = 4.6\times 10^{-3}\,\frac{S(SM)^{\frac{1}{2}}n}{H^{\frac{2}{3}}\nu^{\frac{2}{3}}f^{\frac{1}{3}}}, \tag{4.5}$$

$$r_{\min} = 7.5\times 10^{-6}\,\frac{f^{\frac{2}{3}}H^{\frac{4}{3}}}{\nu^{\frac{2}{3}}}, \tag{4.6}$$

whereas α becomes

$$\alpha = 5.8\,\frac{\nu^{\frac{1}{3}}H^{\frac{1}{3}}f^{\frac{1}{6}}}{n^{\frac{1}{2}}[S(SM)^{\frac{1}{2}}]^{\frac{1}{6}}}. \tag{4.7}$$

The error bars delimiting these values of r are shown in figure 2 for three experimental conditions studied by HBG. The scale of the most unstable mode (for $A < 1$) is one fourth of the typical lengthscale of eddy spacing, so that the scaling of our model is the correct order of magnitude for determining the scale of the steady vortices observed in the experiments. This was not an obvious result *a priori* with

regard to the very large values of the Taylor number. On the other hand the critical Reynolds numbers for the onset of instability are, in general, one order of magnitude larger than the Reynolds numbers in the experiment. This discrepancy is presumably a result of the closure of the turbulent kinetic energy which was chosen to be as simple as possible.

Turning our attention to the experiments of Colin de Verdière (1980), the corresponding values of $r_{\max}$, $r_{\min}$ and α have been computed and are also plotted in figure 2. Rossby numbers are smaller in these experiments than in HBG's. The wavenumbers α for the experimental conditions correspond approximately to the one observed by HBG, but the range of Reynolds numbers $r_{\min} \leqslant r \leqslant r_{\max}$ are lower compared with HBG conditions. The comparison with our model is, however, apparently unsuccessful. Colin de Verdière did not study in detail the vortex structures, but his vortices seem also to be quasi-steady vortices.

The model implies the existence of a flow regime, for sufficiently low values of $2\langle w_b^2\rangle H^2/\nu^2$, that is stable. This regime, analogous to the conductive state in Rayleigh–Bénard convection, only displays turbulent eddies having a timescale of the order of magnitude of the turbulent turnover time. This regime was not observed in the experiments. Indications on how to establish a turbulent flow without the occurrence of steady vortices follow from (4.5). If such a flow regime exists according to the present theory, it should be observed when decreasing the value of r. This cannot be done by decreasing the frequency n of the grid oscillation because turbulence is already weak in HBG experiments (the Reynolds number based on the integral lengthscale is proportional to n and of the order of magnitude of 600). Moreover, the depth H cannot be increased significantly in any experimental facility (the depth of the HBG tank is 80 cm) and there would be serious doubts about the establishment of a quasi-geostrophic turbulent flow in a much deeper layer. The best choice is presumably to increase the rotation rate of the tank. Equation (4.7) implies that the eddy spacing of the vortices will then decrease†.

The discussion above neglected the eddy diffusivity ν_t introduced in the closure of the turbulent kinetic energy equation. Taking this eddy diffusivity into account, the experimental points in figure 2 would then be displaced to smaller values of r and larger values of α, but the effect could not be very important, as Colin de Verdière (1980) and Mory & Hopfinger (1985) measured relatively low eddy viscosities.

A number of discrepancies between the results predicted by the model and experimental observations highlight its weaknesses. First, coherent eddies in the experiments are not geostrophic, at least inside the vortex cores which are of limited extent compared to the eddy spacing. The model is linear and geostrophic, implying a much larger size of the vortex cores and much smaller strengths. Secondly, the normal mode analysis seeks out solutions that consist of an array of cyclonic and anticyclonic vortices. Video films of HBG experiments show that both cyclonic and anticyclonic vortices are generated when turbulence is suddenly produced in a rotating tank, but cyclonic vortices are quickly enhanced, producing strong shears which destroy the anticyclonic vortices. The steady-state pattern in the experiments thus consists of an array of cyclonic vortices, the anticyclonic vorticity being distributed in between them. Colin de Verdière's experiments give qualitatively

† The only useful information to be obtained from the experiments comes from qualitative observations of the flow field. In particular, a quantitative measurement of the mean flow, by introduction of a hot-film probe or LDA measurements, is not possible. The evolution timescales of the quasi-steady vortices are up to 100 rotation periods of the tank, and this is not a sufficient duration to distinguish the steady and the fluctuating components of the velocity signal.

better 'test flows' for the theory, because anticyclonic and cyclonic vortices are in equal number, and vorticity apparently is smaller than in HBG's. (Colin de Verdière did not, however, measure the vorticity inside the vortices.)

5. Conclusion

The most important limitation of the model is the necessary recourse to a closure theory of the turbulent kinetic energy equation. Section 4 brought out the difficulties of a quantitative comparison between the model and the experiments. However, in spite of the evidence given by the experiments, that ageostrophic and nonlinear processes are an important part of the dynamics, and in spite of the speculative nature of the study due to the numerous assumptions of the theory, the linear model presented in this paper captures some of the major features of the experiments that were not given by the previous theories, especially theories relating the vortex genesis to the angular-momentum mixing (Bretherton & Turner 1968; McEwan 1976; Thompson 1979). First, the model provides an explanatory framework for the steadiness of the coherent vortices generated, an observation that no earlier model has accounted for, as far as we know. Secondly, the eddy spacing in the experiment is of the order of magnitude of the scales for which the model predicts an instability to occur. Thirdly, the critical numbers for the onset of instability are one order of magnitude larger than the values achieved in the experiments. This is not a very significant disagreement since the closure remains very crude. A fourth crucial feature of the model is that the occurrence of vortices depends only on the dynamics of the layer. Some flow is allowed between the layer and the outside, but the dynamics of the exterior (not described here) take no part in the generation of this flow. This flow ensures stretching in order to overcome viscous dissipation of the vortices. The existence of such a flow was a starting point for the theories of Maxworthy *et al.* (1985) and Lundgren (1985), whereas it is a consequence of the dynamics of the quasi-geostrophic layer in our model.

Since the pioneering work of Malkus (1956) it has been often considered that the occurrence of turbulence in an unstable flow tends to modify the mean profiles (velocity or temperature) so that the resulting mean flow is marginally unstable with regard to the instability at work. To mention only part of the literature, we cite the cases of Poiseuille or Taylor–Couette flows (Malkus 1978), Rayleigh–Bénard layers (Spiegel 1961) and jets, wakes and shearing layers (Lessen 1978). Such a mechanism may happen even for very highly supercritical conditions, and Barcilon *et al.* (1978) observed that a Taylor–Couette flow having very high Taylor numbers returns in certain conditions to a marginally unstable flow pattern. Our work places a particular emphasis on the marginally unstable conditions by conjecturing that the vortex flow corresponds to a marginally unstable flow pattern, and is therefore connected to the previously cited works. However, our approach differs from that of Malkus in a number of ways. The first is that Malkus' ideas were applied to flows where turbulence is a result of a well-identified instability. The criterion for instability is well established and the mean profiles have very simple geometrical properties (one-dimensional for Poiseuille flows, for instance). In turbulent rotating flows such as those considered here, turbulence is not produced by a simple instability mechanism and the geometry is rather complicated. Our work can only be a necessary first step towards a theory inspired by Malkus' ideas, as it is the first one to propose an instability mechanism in turbulent rotating flows. A second problem is a basic contradiction between one of our assumptions and one of Malkus'. A major

hypothesis of Malkus' theory, which greatly simplifies the modelling of turbulence, is to neglect any modification of turbulence when an instability occurs. The instability only depends on the mean flow pattern. Recall that our theory has its origin in the opposite assumption (see (3.3)).

We have demonstrated the analogy in a rotating fluid between thermal convection and turbulence, arising from the similarity between temperature in thermal convection and the gradient along the rotation axis of the turbulent kinetic energy in quasi-geostrophic turbulence. Another type of instability could have been evoked to explain the vortex genesis. The analogy between stratification and rotation has been often mentioned, but Veronis (1967) pointed out major differences between the two. In particular, a formal analogy is certainly difficult to establish between turbulence in a stratified flow (Ivey & Corcos 1982; Browand & Hopfinger 1985) and turbulence in a rotating fluid. The latter authors explained the formation of mixed layers in a stratified turbulent flow by an argument based on conversion of kinetic energy into potential energy. It is not obvious how to express a quantity in a rotating fluid that is equivalent to potential energy in a stratified flow. Thermal convection is a phenomenon which is closer to quasi-geostrophic turbulence than are stratified turbulent flows.

E. J. Hopfinger is gratefully acknowledged for his support. Discussions with J. Brougham, M. Lesieur, T. Maxworthy, P. Vincent, J. Wells and, in particular, P. Huerre and J. Sommeria have been of crucial importance. We are indebted to J. C. R. Hunt, associate editor of *JFM*, who pointed out a possible relation of our work with previous studies on the marginal stability of turbulence shear flows. The work was financially supported by the ATP 'Fluides Géophysiques et Astrophysiques' under contract IFREMER no. 9433.

REFERENCES

Barcilon, A., Brindley, J., Lessen, M. & Mobbs, F. R. 1979 *J. Fluid Mech.* **94**, 453–463.

Bretherton, F. P. & Turner, J. S. 1968 *J. Fluid Mech.* **32**, 449–464.

Browand, F. K. & Hopfinger, E. J. 1985 In *IMA Conf. Proc. Cambridge, 1983*. Clarendon.

Chandrasekhar, S. 1961 *Hydrodynamics and Hydromagnetics Stability*. Dover.

Colin de Verdière, A. 1980 *Geophys. Astrophys. Fluid Dyn.* **15**, 213–251.

Dickinson, S. C. & Long, R. R. 1982 *J. Fluid Mech.* **126**, 315–333.

Hopfinger, E. J., Browand, F. K. & Gagne, Y. 1982 *J. Fluid Mech.* **125**, 505–534.

Ivey, G. N. & Corcos, G. M. 1982 *J. Fluid Mech.* **121**, 1–26.

Lessen, M. 1978 *J. Fluid Mech.* **88**, 535–540.

Lundgren, T. S. 1985 *J. Fluid Mech.* **155**, 381–412.

McEwan, A. D. 1976 *Nature* **260**, 126–128.

Malkus, W. V. R. 1956 *J. Fluid Mech.* **1**, 521–539.

Malkus, W. V. R. 1978 *J. Fluid Mech.* **90**, 401–414.

Maxworthy, T., Hopfinger, E. J. & Redekopp, L. 1985 *J. Fluid Mech.* **151**, 141–165.

Monin, A. S. & Yaglom, A. M. 1965 *Statistical Fluid Mechanics*. MIT Press.

Morse, P. M. & Feshbach, H. 1953 *Methods of Theoretical Physics*. McGraw Hill.

Mory, M. & Hopfinger, E. J. 1985 In *Macroscopic Modelling of Turbulent Flows*, Lecture Notes in Physics, vol. 230, Springer.

Mory, M. & Hopfinger, E. J. 1986 *Phys. Fluids* **29**, 2140–2146.

Nakagawa, Y. & Frenzen, P. 1955 *Tellus* **7**, 1–21.

Pedlosky, J. 1979 *Geophysical Fluid Dynamics*. Springer.

RHINES, P. B. 1979 *Ann. Rev. Fluid Mech.* **11**, 401–441.
SCORER, R. S. 1966 *Science* **2**, 46–52.
SPIEGEL, E. A. 1961 In *Mecanique de la Turbulence*, p. 181. Marseille: CNRS.
THOMPSON, R. O. R. Y. 1979 *Geophys. Astrophys. Fluid Dyn.* **12**, 221–223.
VERONIS, G. 1959 *J. Fluid Mech.* **5**, 401–435.
VERONIS, G. 1967 *Tellus* **19**, 326–335.